Available online at http://scik.org

Commun. Math. Biol. Neurosci. 2025, 2025:143

https://doi.org/10.28919/cmbn/9549

ISSN: 2052-2541

MATHEMATICAL MODELLING OF MICROBIAL-NUTRIENT KINETICS IN BIOCHAR AMENDED SOILS USING BACKWARD DIFFERENTIATION FORMULA

OLUSEGUN ADEYEMI OLAIJU[1], JOSHUA KAYODE ODEYEMI[1,*], MUKAIL AKINDE[2], OLASUNKANMI OLAPEJU[3], FOLAKEMI MARGARET OKAFOR[4]

[1]Department of Mathematics, The Federal Polytechnic Ilaro, Ogun State, Nigeria

[2]Department of Taxation, Federal Polytechnic Ilaro, Ilaro, Ogun State, Nigeria

[3]Department of Urban and Regional Planning, The Federal Polytechnic Ilaro, Ogun State, Nigeria

[4]Department of Mathematics Programme, National Mathematical Centre Abuja, Abuja, Nigeria

Abstract: Soil degradation and nutrient depletion pose significant challenges to sustainable agriculture, especially in intensively farmed areas with low organic matter inputs. The use of biochar in farmlands with minimal organic matter inputs aims to sequestrate carbon while also improving soil fertility, microbial activity, and crop yield. Microbial growth, governed by nutrient-mediated kinetics, crucial for soil health and productivity, is largely absent from current land surface models used in climate mitigation assessments. Here, to fill this gap, this study formulated a mathematical model that incorporates nonlinear microbial growth and nutrient uptake kinetics modulated by biochar, capturing feedback loops that influence soil health and productivity. An implicit technique that works especially well for stiff ODEs, the Backward Differentiation Formula (BDF), was used to solve the system in order to guarantee numerical stability and computational efficiency. The model's sensitivity analysis was evaluated using both the Morris and Sobol techniques to determine which factors had a significant impact on nutrient-driven microbial growth dynamics and consequent soil health outcomes. The Morris method revealed that microbial carrying capacity (M_{Max}) and crop growth efficiency (β) exert direct effects on yield, as indicated by high mean elementary effects (μ^*). Meanwhile, the Sobol analysis confirmed M_{Max} as the most influential parameter via its high first-order index $(S_1 \approx 0.38)$, while the total-order index (S_T) highlighted β and crop decay rate (d_Y) as critical drivers through their interaction

*Corresponding author

E-mail address: joshua.odeyemi@federalpolyilaro.edu.ng

Received August 13, 2025

effects ($S_T \approx 0.42$). The convergence of both methods on M_{Max} as the primary determinant reinforces its central role in regulating microbial biomass and productivity. Discrepancies, such as $\beta's$ low S_1 but high S_T, underscore the importance of considering parameter interactions. These findings demonstrate the value of integrating elementary effect and variance-based methods to enhance model simplification and inform targeted agricultural decision-making.
Keywords: microbial-nutrient kinetics; crop yield; biochar; biochar-amended soils.
2020 AMS Subject Classification: 92D25, 92C45, 65L06.

1. INTRODUCTION

Biochar soil amendments have attracted significant attention for improving soil fertility and increasing soil carbon reserves. The use of biochar to improve soil fertility and sequester carbon in the soil has been implemented in the Amazon region in recent years [1, 2, 3]. Given its long-term sustainability, affordability, and environmental impact, biochar offers a strong substitute for conventional soil amendments such as compost and chemical fertilisers [1, 2, 4, 5]. Biochar is a close substitute for sustainable farming practices due to its properties, which reduce greenhouse gas emissions and enhance soil health [6, 7, 45]. Consequently, it improves soil structure, retains more water, and fosters microbial diversity—all of which are essential for sustained soil fertility. However, some soil carbon and nutrient models treat biochar as a static amendment—an inert carbon pool with set properties—despite an increasing amount of experimental evidence, because it is generally considered resistant to decomposition and microbial degradation compared to other soil organic matter [8, 9, 10, 11]. This simplification ignores the dynamic relationships that support important feedbacks in soil ecosystems, such as those between biochar, nutrient availability, and microbial growth. Meanwhile, the degradation of soil organic matter is predicted by traditional models such as CENTURY and RothC, which employ first-order kinetics rather than explicitly representing microbial biomass [12, 13, 14].

Microbial carbon cycling has been better understood, even with more recent microbial-explicit models such as MIMICS and CORPSE [15, 16], which have not taken into account changes brought about by biochar in terms of microbial growth rates, nutrient uptake efficiency, or microbial community structure. The Michaelis-Menten-type formulations, which depict critical biogeochemical processes as microbial substrate utilisation and plant nutrient acquisition, have recently been employed in microbial-plant feedback models to investigate nutrient absorption kinetics and microbial development [12, 72, 73]. However, a critical limitation of these existing models either ignore biochar totally or approach it as a static input with fixed effects (e.g., a one-

time boost to nutrient retention or pH adjustment) [10, 11, 73, 74], failing to account for the time-dependent interactions between biochar and soil biota including gradual aging, microbial colonisation, surface oxidation, and evolving impacts on nutrient availability and carbon stabilisation. To address these gaps, this study proposes a system of coupled nonlinear differential equations that explicitly connect the microbial growth (represented by nutrient-mediated Monod kinetics), nutrient dynamics (including replenishment and uptake), the modulatory effects of biochar on microbial efficiency and nutrient retention, and aggregate soil health indices as emergent properties of microbial–nutrient interactions.

Meanwhile, models that explicitly depict biochar as a dynamic state variable [6, 7, 75, 76, 77] present nonlinear feedbacks and multiple temporal scales. In particular, rapid microbial responses (hours to days) and slow biochar decay (months to years) continuously affect microbial activity, nutrient retention, and soil carbon accumulation. This results in a stiff system where the step-size limits make ordinary explicit solutions computationally prohibitive. To overcome these problems, numerical methods have become widespread in large-scale biogeochemical modelling. To model long-term carbon and nitrogen dynamics, for example, the CENTURY model [13, 14, 78], DNDC (DeNitrification-DeComposition) [79, 80], DayCent, ECOSSE (Estimating Carbon in Organic Soils - Sequestration and Emissions), and the MAGIC (Model of Acidification of Groundwater In Catchments) [81] rely on implicit integration schemes. Among these, the efficient and stable BDF has emerged as a numerical method for solving stiff ordinary differential equations (ODEs). BDF methods are implicit linear multistep algorithms that use previously calculated variables to approximate the solution of ODEs.

Adopting a BDF makes it possible to simulate feedback loops, such as how microbial development is restricted by nutrient depletion and how biochar improvement increases nutrient-use efficiency, both of which have an impact on soil productivity. Also, the model identifies important factors of agricultural yield while reducing parameter dimensionality by using global sensitivity analysis using the Morris and Sobol techniques. Morris screening and Sobol variance-based approaches are complementary strategies used to improve model building and reduce parameter uncertainty, necessitating sensitivity analysis. To identify important parameters in an efficient, one-at-a-time (OAT) manner, the Morris screening method analyses the mean (μ^*) and variability (σ) of elementary effects [69, 70, 71, 82]. In contrast, the Sobol variance-based method divides output variance into first-order and total-order effects, capturing direct and interaction-driven influences

[69, 70, 71, 83, 84]. Morris has been used to prioritize parameters in microbial and nutrient submodels in agroecosystems [85], whereas Sobol has been used to assess climatic, soil, and management uncertainty in crop models such as APSIM and AquaCrop [86, 87].

This study combines two methods to quantify the importance of parameters like baseline microbial growth rate, nitrogen uptake efficiency, and nitrogen input. It also highlights strong interaction effects in parameters like nutrient saturation constants, where high but low values indicate context-dependent dynamics not seen in simpler models.

2. MATERIALS AND METHODS

2.1 MODEL FORMULATION

We formulated a set of nonlinear ordinary differential equations (ODEs) to model the dynamic interactions between soil nutrients, microbial biomass, biochar decomposition, soil carbon, and plant biomass, capturing the time-dependent behavior of the soil and plant system components listed below. The model includes microbial growth influenced by nutrient availability and biochar, nutrient absorption, leaching, and biochar-mediated retention, soil carbon dynamics through microbial activity and biochar, and plant development influenced by microbial activity and nutritional sufficiency. Table 1 lists the state variables, biological characteristics, and environmental parameters that controlled the system.

Model Assumptions

1. Biochar affects microbial growth by improving habitat, pH, and nutrient retention.
2. Microbial biomass responds to nutrient availability and decays naturally.
3. Crop yield is a function of both nutrient availability and microbial support.

Table 1

Variable	Description
$\boldsymbol{M(t)}$	Microbial biomass (mg/g soil)
$\boldsymbol{N(t)}$	Nitrogen concentration (mg N/L)
$\boldsymbol{P(t)}$	Phosphorus concentration (mg P/L)
$\boldsymbol{C_s(t)}$	Soil organic carbon (mg C/g soil)
$\boldsymbol{B(t)}$	Biochar amount (mg/g soil)
$\boldsymbol{Y(t)}$	Crop yield (unitless)

Parameter	Description
$\boldsymbol{\mu_0}$	Max microbial growth rate (day^{-1})
$\boldsymbol{\alpha_B}$	Influence of biochar on growth Natural death rate
$\boldsymbol{\alpha_N}$	N uptake rate by microbes (mg N/g M/day)
$\boldsymbol{\alpha_P}$	P uptake rate by microbes (mg P/g M/day)
$\boldsymbol{K_N, K_P}$	Half-saturation constants for N and P
$\boldsymbol{M_{\max}}$	Max microbial biomass (mg/g soil)
$\boldsymbol{d_M}$	Microbial decay rate (day^{-1})
$\boldsymbol{I_N, I_P}$	Input rates of nitrogen and phosphorus (mg/L/day)
$\boldsymbol{U_N, U_P}$	Uptake rates of N and P (day^{-1})
$\boldsymbol{L_N, L_P}$	Leaching rates of N and P (day^{-1})
$\boldsymbol{k_B}$	Decay rate of biochar effect (day^{-1})
$\boldsymbol{r_M}$	Microbial respiration rate (day^{-1})
$\boldsymbol{d_C}$	Carbon loss rate (day^{-1})
$\boldsymbol{\beta}$	Crop carbon-use efficiency
$\boldsymbol{K_Y}$	Yield saturation constant
$\boldsymbol{d_Y}$	Crop yield decay rate (day^{-1})

2.1.1 MICROBIAL BIOMASS DYNAMICS

The growth of microbial communities in soil is not permanent. They grow according to a realistic biological pattern instead. When populations are small, microbes reproduce by exploiting the available resources, resulting in rapid (near-exponential) increases. There is competition when microbial biomass increases because additional space, energy, and nutrients are needed. As the population reaches the carrying capacity of the ecosystem, this density-dependent restriction inhibits growth. Not every bacterium escapes this process; some die as a result of environmental stress, viral lysis, or predation, which results in the elimination of the biomass from the system by this mortality. Microbial dynamics are therefore controlled by a balance between turnover/mortality, crowding effects (logistic limitation), and stimulation (by biochar and nutrients). Let $M(t)$ be the microbial biomass (in mg C kg^{-1} soil) at time t. The rate of change of microbial biomass is governed by the following ordinary differential equation:

$$\frac{dM}{dt} = \mu M\left(1 - \frac{M}{M_{\max}}\right) - d_M M,\ M(0) = M_0 \quad (1)$$

where $\mu M\left(1 - \frac{M}{M_{\max}}\right)$ is the density-dependent growth that declines as M approaches $M_{\max}$, while $-d_M M$ is the linear loss proportional to biomass. Thus, the net per-capita growth rate is:

$$\frac{1}{M}\frac{dM}{dt} = \mu\left(1 - \frac{M}{M_{\max}}\right) - d_M \quad (2)$$

The population increases when $\mu\left(1 - \frac{M}{M_{\max}}\right) > d_M$ and decreases otherwise.

2.1.2 NUTRIENT DYNAMICS (NITROGEN & PHOSPHORUS)

Microbial activity, sustainable agricultural output, and ecosystem productivity depend on the availability of nitrogen (N) and phosphorus (P) in the soil. These nutrients enter the soil system through external inputs, represented as input fluxes I_N and I_P. These inputs include atmospheric deposition (especially for N), mineralisation of organic materials, and synthetic or organic fertilisation. Proteins (N-rich), DNA/RNA (N and P), ATP (P-rich), and cell membranes (P in phospholipids) all depend on nitrogen and phosphorus, which microbes scavenge from the soil as their biomass M grows. When microbes die, these nutrients are released back (via turnover), but not instantly. Since microbial growth and nutrient demand are closely related, microbial uptake is proportional to biomass (M), with rate coefficients U_N and U_P representing the average cellular requirements and uptake efficiency of the species in ambient conditions.

Concurrently, a sizable portion of the available nutrients is susceptible to loss pathways that restrict their agronomic utility and retention. While phosphorus loss pathways are runoff (attached to soil particles), erosion, or chemical fixation (bound to iron/aluminium/clay) into unavailable mineral forms, nitrogen is especially vulnerable to leaching (as nitrate), gaseous losses via denitrification, and volatilisation. The dependence of the magnitude of the loss on the current nutrient concentration is captured by parameterising these biotic and abiotic removal processes as first-order loss terms $L_N N$ and $L_p P$.

In this study, our model uses a saturation-type retention function to account for the dynamic influence of biochar instead of treating it as a static amendment:

$$\left(1 - \frac{\alpha_B B}{B + K_X}\right), X \in \{N, P\}$$

This formulation represents the diminishing marginal returns observed in empirical systems: at low biochar concentrations ($B \ll K_X$), nutrient protection increases nearly linearly with B; at high

concentrations, the effect plateaus due to site saturation. The parameter α_B $(0 \leq \alpha_B \leq 1)$ quantifies the maximum proportional reduction in loss rate achievable by biochar, while K_X denotes the biochar concentration at which half of this maximum effect is achieved, similar to a half-saturation constant in enzyme kinetics. Thus, biochar-induced inputs, biological uptake, abiotic losses, and retention form a controlled subsystem that regulates nutrient use efficiency and ecosystem resilience. The following system of ordinary differential equations describes the temporal evolution of the available nitrogen and phosphorus:

$$\frac{dN}{dt} = I_N - U_N M \cdot \frac{N}{N+K_N} - L_N N \left(1 - \frac{\alpha_B B}{B+K_N}\right) \tag{3}$$

$$\frac{dP}{dt} = I_P - U_P M \cdot \frac{P}{P+K_p} - L_P P \left(1 - \frac{\alpha_B B}{B+K_P}\right) \tag{4}$$

2.1.3 SOIL CARBON AND BIOCHAR DYNAMICS

This study models the soil carbon pool (C_s) as a dynamic reservoir impacted by biotic and abiotic inputs, turnover processes, and decomposition losses. For biochar, the net effect of slow biotic and abiotic breakdown is called a first-order decay process $(dB/dt = -k_B B)$. The released carbon moves at a rate of $k_B B$ into the soil carbon pool. This single-pool first-order formulation provides a concise representation suitable for ecosystem-scale modelling, although the actual decomposition of biochar may involve multiple pools and mechanisms. At the same time, microbial biomass turnover contributes to the soil carbon pool, labile and semi-labile organic wastes, such as necromass, cell fragments, and extracellular polymeric substances [16, 17]. These microbial-derived inputs are gaining acceptance as key precursors to stable soil organic matter. This pathway is indicated in the current model by the term $r_M M$, where M is the active microbial biomass and r_M is the carbon conversion efficiency from microbial biomass to persistent soil carbon. The heterotrophic respiration of organic substrates at a rate $d_C C_s$ drives mineralisation losses, which offset the accumulation of C_s. The overall impact of microbial utilisation and enzymatic breakdown of soil organic carbon is captured by this first-order flux term, which is indirectly impacted by environmental factors through their influence on microbial activity. The governing equations for the dynamics of the carbon pool and the degradation of biochar are given below:

$$\frac{dC_s}{dt} = k_B B + r_M M - d_C C_s \tag{5}$$

$$\frac{dB}{dt} = -k_B B \tag{6}$$

2.1.4 CROP YIELD DYNAMICS

Using two crucial ecological concepts—Michaelis-Menten kinetics and Liebig's Law of the Minimum—the crop yield (Y) is modelled as a dynamic state variable whose rate of change depends nonlinearly on microbial biomass (M) and the availability of nitrogen and phosphorus (see [18, 19]).

Additionally, based on key nutrient thresholds, we develop a switching condition to account for physiological thresholds below which plant growth is effectively restricted. The growth rate is set to zero when either N or P drops below 10% of the half-saturation constant K_Y. This threshold mechanism reflects the scientific observation that plants require a minimum level of nutrients to begin growing efficiently and prohibits biologically implausible development under extremely inadequate conditions [20]. In addition, microbial biomass (M) acts as a key driver of yield potential, scaling the maximum possible growth rate. The resulting formulation yields a piecewise differential equation that governs the temporal evolution of crop yield, combining threshold-driven activation with nutrient co-limitation and microbial mediation. The following governing equation for crop yield dynamics is given below:

$$\frac{dY}{dt} = \begin{cases} 0, & \text{if } N < 0.1K_Y \text{ or } P < 0.1K_Y \\ \beta M \cdot \frac{N}{N+K_Y} \cdot \frac{P}{P+K_Y} - d_Y Y, & \text{otherwise} \end{cases} \tag{7}$$

2.1.5 THE COUPLED SYSTEM OF ODES

The coupled system of ODEs of Eqs. 1, 3, 4, 5, 6, and 7 is as follows:

$$\begin{aligned} \frac{dM}{dt} &= \mu M\left(1 - \frac{M}{M_{\max}}\right) - d_M M \\ \frac{dN}{dt} &= I_N - U_N M \cdot \frac{N}{N+K_N} - L_N N\left(1 - \frac{\alpha_B B}{B+K_N}\right) \\ \frac{dP}{dt} &= I_P - U_P M \cdot \frac{P}{P+K_p} - L_P P\left(1 - \frac{\alpha_B B}{B+K_P}\right) \\ \frac{dC_s}{dt} &= k_B B + r_M M - d_C C_s \\ \frac{dB}{dt} &= -k_B B \\ \frac{dY}{dt} &= \begin{cases} 0, & \text{if } N < 0.1K_Y \text{ or } P < 0.1K_Y \\ \beta M \cdot \left(\frac{N}{N+K_Y}\right) \cdot \left(\frac{P}{P+K_Y}\right) - d_Y Y, & \text{otherwise} \end{cases} \end{aligned} \tag{8}$$

where μ depicts the effective microbial growth rate which is defined by:

$$\mu = \mu_0 + \alpha_B B + \alpha_N \cdot \frac{N^2}{K_N^2+N^2} + \alpha_P \cdot \frac{P^2}{K_P^2+P^2} b \tag{9}$$

Subjected to the following initial conditions defined for all the state variables:

$$M(0) = 10.0, N(0) = 10.0, P(0) = 5.0,$$
$$C_s(0) = 20.0, Y(0) = 5.0,$$
$$B(0) = \begin{cases} 30.0 & \text{(with biochar)} \\ 0.0 & \text{(without biochar)} \end{cases} \tag{10}$$

2.2 BACKWARD DIFFERENTIATION FORMULA

In this section, we provided a numerical technique for solving the soil-plant-biochar system of nonlinear ordinary differential equations (ODEs) with the potential stiffness of the system (fast microbial dynamics vs. delayed nutrient decay) using the Backward Differentiation Formula.

Let the state vector be:

$$\mathbf{y}(t) = \begin{bmatrix} M(t) \\ N(t) \\ P(t) \\ C_s(t) \\ B(t) \\ Y(t) \end{bmatrix} \tag{11}$$

The system is defined as:

$$\frac{d\mathbf{y}}{dt} = \mathbf{f}(t, \mathbf{y}) \tag{12}$$

where $\mathbf{f}$ is determined by the equations, and the microbial growth rate μ given by:

$$\mu = \mu_0 + \alpha_B B + \alpha_N \cdot \frac{N^2}{K_N^2 + N^2} + \alpha_P \cdot \frac{P^2}{K_P^2 + P^2} \tag{13}$$

For a scalar function $y(t)$ using the general k-step BDF method, we have

$$\sum_{j=0}^{k} \alpha_j y_{n-j} = h \cdot \beta f(t_n, y_n) \tag{14}$$

where h is the time step, y_n is the approximate solution at time t_n, and α_j, β are method-dependent constants. We solved this implicitly at each time step t_n, since y_n appears on both sides. With f_1 representing $M(t)$, f_2 representing Nitrogen $N(t)$, f_3 representing $P(t)$, f_4 representing $C_s(t)$, f_5 representing $B(t)$, and f_6 representing $Y(t)$, we have now defined f componentwise below.

$$\begin{aligned} f_1 &= \mu M \left(1 - \frac{M}{M_{\max}}\right) - d_M M \\ f_2 &= I_N - U_N M - L_N N \left(1 - \frac{\alpha_B B}{B + K_N}\right) \\ f_3 &= I_P - U_P M - L_P P \left(1 - \frac{\alpha_B B}{B + K_P}\right) \\ f_3 &= I_P - U_P M - L_P P \left(1 - \frac{\alpha_B B}{B + K_P}\right) \\ f_5 &= -k_B B \\ f_6 &= \begin{cases} 0, & \text{if } N < 0.1K_Y \text{ or } P < 0.1K_Y \\ \beta M \cdot \left(\frac{N}{N + K_Y}\right) \cdot \left(\frac{P}{P + K_Y}\right) - d_Y Y, & \text{otherwise} \end{cases} \end{aligned} \tag{15}$$

We discretized the BDF-1 System using the Backward Euler method because of its A-stability, which is helpful for stiff ODEs. Let $\mathbf{y}_n \in \mathbb{R}^6$ be the state vector at time t_n, with step size h. The backward Euler step is:

$$\mathbf{y}_n = \mathbf{y}_{n-1} + h \cdot \mathbf{f}(t_n, \mathbf{y}_n) \tag{16}$$

with each state variables, we have:

$$\begin{aligned} M_n &= M_{n-1} + h \cdot f_1(t_n, \mathbf{y}_n) \\ N_n &= N_{n-1} + h \cdot f_2(t_n, \mathbf{y}_n) \\ P_n &= P_{n-1} + h \cdot f_3(t_n, \mathbf{y}_n) \\ C_{s,n} &= C_{s,n-1} + h \cdot f_4(t_n, \mathbf{y}_n) \\ B_n &= B_{n-1} + h \cdot f_5(t_n, \mathbf{y}_n) \\ Y_n &= Y_{n-1} + h \cdot f_6(t_n, \mathbf{y}_n) \end{aligned} \tag{17}$$

And the above nonlinear equations in $\mathbf{y}_n$ are solved simultaneously via Newton-Raphson at each time step. We fixed the simulation interval to be $[0, T]$, with $N = 500$ evenly spaced steps which is given below:

$$h = \frac{T}{N} \text{ and } t_n = nh \tag{18}$$

2.3 SENSITIVITY ANALYSIS

For the parameter space and perturbation bounds, each model parameter p_i is varied within:

$$p_i \in [0.5p_i^{\text{base}}, 1.5p_i^{\text{base}}] \tag{19}$$

The input domain for sensitivity analysis is defined by Eq. (19). We used Sobol Global Sensitivity Analysis for quantitative variance decomposition and Morris Screening for qualitative screening. For Morris method, the input space normalized to $[0,1]^d$ and discretized into p levels, while for each parameter i, we computed the elementary effect (EE):

$$EE_i = \frac{f(\theta_1, \ldots, \theta_i + \Delta, \ldots, \theta_d) - f(\theta)}{\Delta} \tag{20}$$

The Eq. (20) is repeated across R random trajectories and the output metrics are μ_i^* (importance) and σ_i (nonlinearity and interactions). Similarly, for Sobol Method, the variance decomposition of model output Y is given by:

$$V(Y) = \sum_i V_i + \sum_{i<j} V_{ij} + \cdots \tag{21}$$

Considering the first-order index we have:

$$S_i = \frac{V_i}{V(Y)} \tag{22}$$

while the total-effect index is given below as:

$$S_{Ti} = 1 - \frac{V_{-i}}{V(Y)} \tag{23}$$

The sampling are based on Saltelli's scheme using $N(2d+2)$ simulations while the outputs of interest include final values of $Y(T)$, $M(T)$, and $C_s(T)$.

3. MAIN RESULTS

This section presents the impacts of applying biochar on soil health, nutrient dynamics, and crop productivity. The impact of applying biochar on the five key soil parameters—crop production, soil carbon (C), microbial biomass, nitrogen (N), and phosphorus (P)—was evaluated. The graph that follows illustrates the dynamic interactions between applying biochar-amended soils over 300 days and contrasting biochar-amended and non-biochar-amended soils. Sensitivity analysis was used to identify critical drivers, and Morris and Sobol demonstrated which parameters had the most influence on the observed patterns. Table 2 shows the parameters and values for the simulation.

Table 2: Parameters (Values for simulation)

Parameter	Values Supported	Model Value	Source	Parameter	Values Supported	Model Value	Source
μ_0	0.08 - 0.09	0.09	[1, 22]	L_N	0.01	0.01	[28, 29]
α_B	0.003 - 0.007	0.007	[23, 24]	I_P	1.0 - 2.5	2.5	[26, 30]
α_N	0.02	0.02	[1, 25]	U_P	0.01	0.01	[26, 30]
α_P	0.015	0.015	[1, 26]	L_P	0.01	0.01	[26, 30]
K_N	10	10.0	[1, 27]	k_B	0.00005 - 0.005	0.00005	[23, 31]
K_P	6	6.0	[26]	r_M	0.02	0.02	[1, 22, 31]
M_{max}	100	100.0	[1, 22]	d_C	0.001-0.005	0.001	[22, 32]
d_M	0.018 - 0.02	0.018	[1, 22, 25]	β	0.1-0.12	0.12	[33]
I_N	2.0 - 4.0	4.0	[28, 29]	K_Y	5	5.0	[33, 34]
U_N	0.01	0.01	[25, 28]	d_Y	0.01	0.01	[33, 35]

Table 3 demonstrates that Backward Differentiation Formula (BDF) was used to predict nutrient dynamics and crop output across soil types over time. The comparative examination of three different soil textures is presented in Table 3, which reveals completely different reactions to the application of biochar.

Table 4 compares a high reference solution for sandy, loamy, and clay soils with the computation times and root mean square errors (RMSE) of three numerical integration schemes: the BDF, traditional fourth-order Runge–Kutta (RK4), and Trapezoidal rule (Trapz).

Table 5 presents the simulation findings, which reveal that the steady-state values for microbial biomass, soil nutrients, soil carbon, biochar, and crop yield were similar across all three numerical approaches (BDF, RK4, and Trapezoidal).

Table 3: Soil and Crop Metrics With vs. Without Biochar Application (BDF-Modeled Data)

	Sandy Soil		Loamy Soil		Clay Soil	
	Biochar	**No Biochar**	**Biochar**	**No Biochar**	**Biochar**	**No Biochar**
Microbial Biomass (mg/g soil)	90.75	91.996	94.576	91.996	97.003	91.996
Nitrogen (mg N/L)	105.115	294.123	292.256	294.123	290.032	294.123
Phosphorus (mg P/L)	9.402	103.909	148.968	103.909	98.964	103.909
Soil Carbon (mg C/g)	476.27	464.185	495.351	464.185	507.488	464.185
Biochar (soil mg/g soil)	29.113	0	29.553	0	29.821	0
Crop Yield	644.742	964.601	1012.83	964.601	1020.185	964.601

Table 4: Computation Time and RMSE of BDF, RK4, and Trapezoidal Methods Compared with Reference Solution for Different Soil Types

	Numerical Integration Schemes				RMSE		
Soil	**Reference Time (s)**	**BDF Time (s)**	**RK4 Time (s)**	**Trapez Time (s)**	**BDF_vs_Ref**	**RK4_vs_Ref**	**Trap_vs_Ref**
Sandy Soil	0.496422052	0.005019903	0.024869919	0.175172091	0.074074487	5.91E-05	0.007714291
Loamy Soil	0.268039465	0.018064737	0.035511494	0.103728294	0.148696841	5.37E-05	0.006347605
Clay Soil	0.311969995	0.016038179	0.017992735	0.125355482	0.146331919	5.63E-05	0.005872083

Table 5: : Simulation Results of Three Numerical Integration Schemes for Microbial biomass, Soil nutrients, Soil carbon, Biochar, and Crop yield

Method	**Microbial Biomass**	**Nitrogen**	**Phosphorus**	**Soil Carbon**	**Biochar**	**Crop Yield**
BDF	85.59807444	300.2377509	157.4824964	431.9355102	-1.50E-14	912.6924536
RK4	85.59489399	300.2884668	157.5075917	431.9237691	1.00E-12	912.9014611
Trapezoidal	85.59489401	300.2888655	157.5078884	431.9199929	1.00E-12	912.9002165

3.1 MICROBIAL BIOMASS (GC/M²) OVER 300 DAYS

Biochar benefits vary with soil texture, with considerable improvements in clay and loamy soils. Figure 1 depicts how the number of live bacteria in soil (measured in carbon) fluctuates over 300 days. Biochar most likely stimulates microbial development by providing habitat and nutrients. The microbial biomass in soils supplemented with biochar achieved a plateau of around 85 gC/m²

in 50 days, while non-biochar soils took almost 150 days to stabilise at approximately 70 gC/m², as shown in Figure 1. Without Biochar, the figure indicated less microbial biomass due to less organic matter.

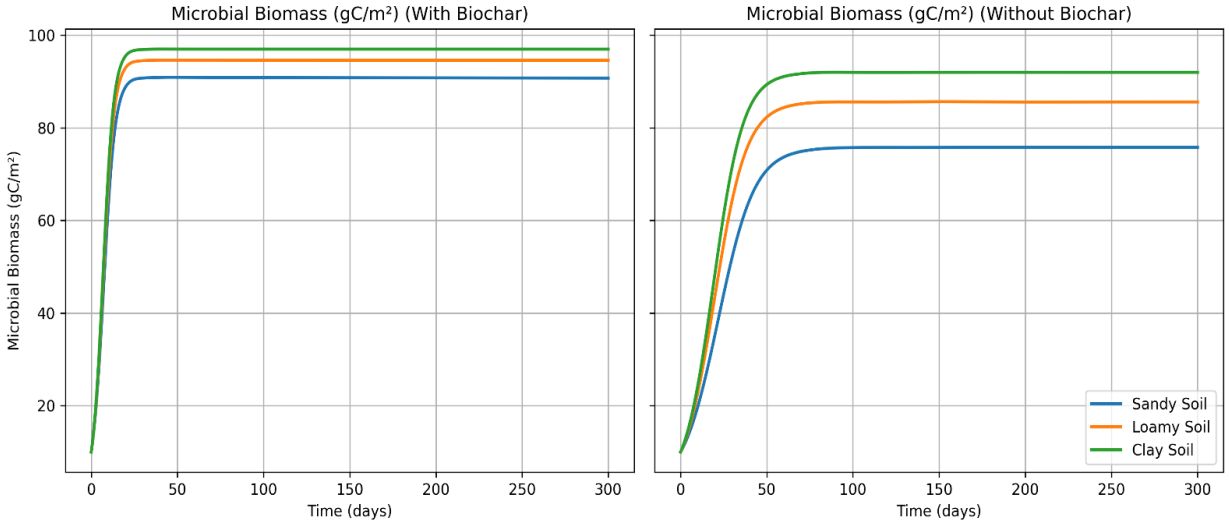

Figure 1: Microbial Biomass (gC/m²) Over 300 Days: BDF-Modeled Trends Showing Enhanced Microbial Growth with Biochar vs. Control

3.2 SOIL NITROGEN (GN/M²) OVER 300 DAYS

Figure 2 demonstrates that Biochar measures nitrogen levels in soil over time. Biochar may hold nitrogen, hence minimizing leaching. Without Biochar, it compares nitrogen levels in sandy, loamy, and clay soils. Nitrogen levels decline quickly, particularly in sandy soil.

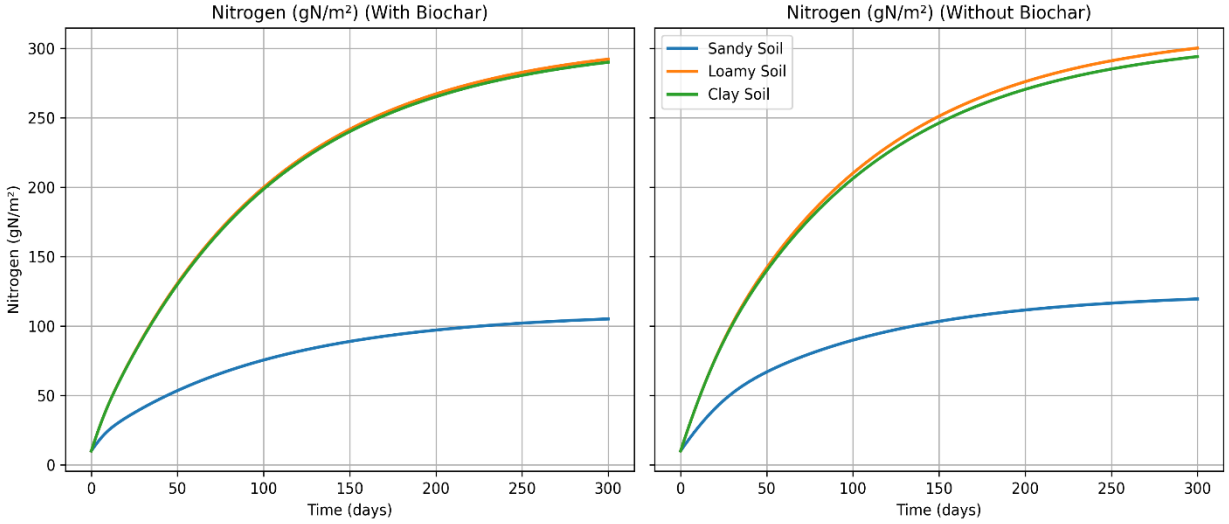

Figure 2: Soil Nitrogen (gN/m²) Dynamics Over 300 Days - BDF-Modeled Trends Showing how Biochar Reduces Nitrogen Loss Across Soil Types with and without Control

3.3 PHOSPHORUS RETENTION (GP/M²) OVER 300 DAYS

Figure 3 shows that Biochar improves phosphorus availability over time by binding nutrients and preventing loss. Without Biochar, phosphorus retention decreases and varies by soil type (clay holds more than sand).

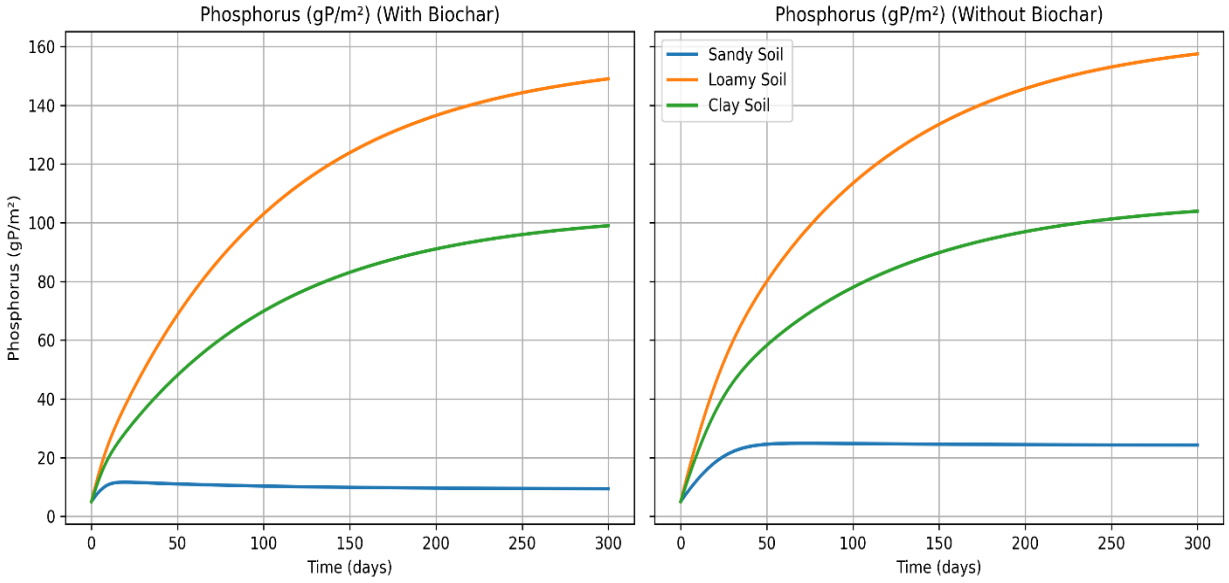

Figure 3: Phosphorus Retention (gP/m²) in Soils Over 300 Days - BDF-Modeled Trends Showing How Biochar Improves Availability Over Time with and without Control

3.4 SOIL CARBON (GC/M²) ACCUMULATION OVER 300 DAYS

Figure 4 shows that with biochar, soil carbon slowly increases as biochar contributes stable carbon, boosting soil fertility, whereas, without biochar, carbon levels decrease, particularly in sandy soils.

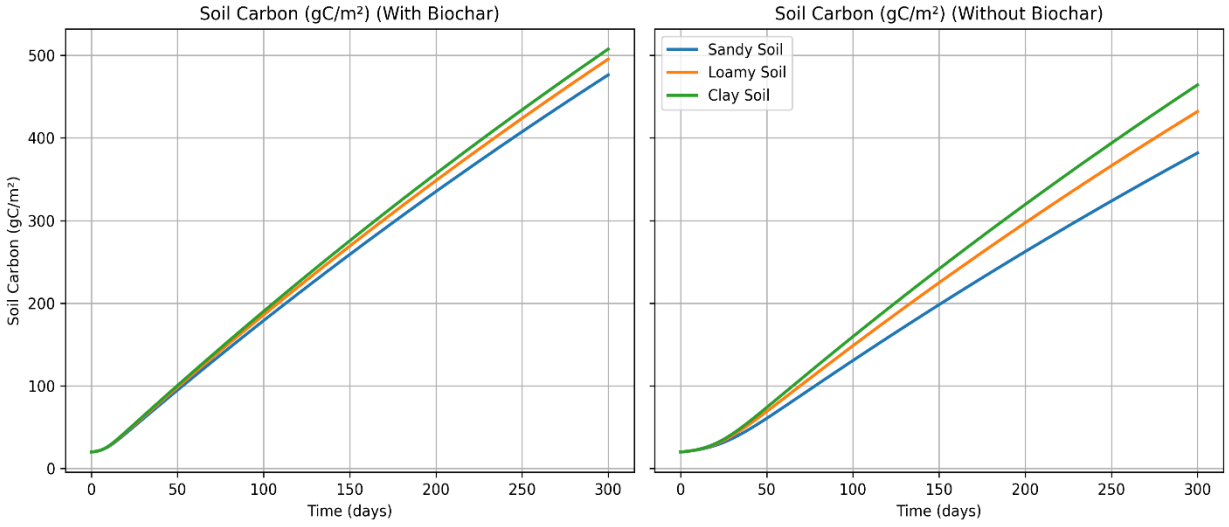

Figure 4:Soil Carbon (gC/m²) Accumulation Over 300 Days: BDF-Modeled Trends Showing the Long-Term Stability with Biochar Application with and without Control

3.5 BIOCHAR PERSISTENCE (G/M²) IN SOIL OVER 300 DAYS

Figure 5 depicts how much Biochar stays in the soil over time after its application. It degrades slowly over months. According to this graph, no biochar was used for 300 days (baseline comparison).

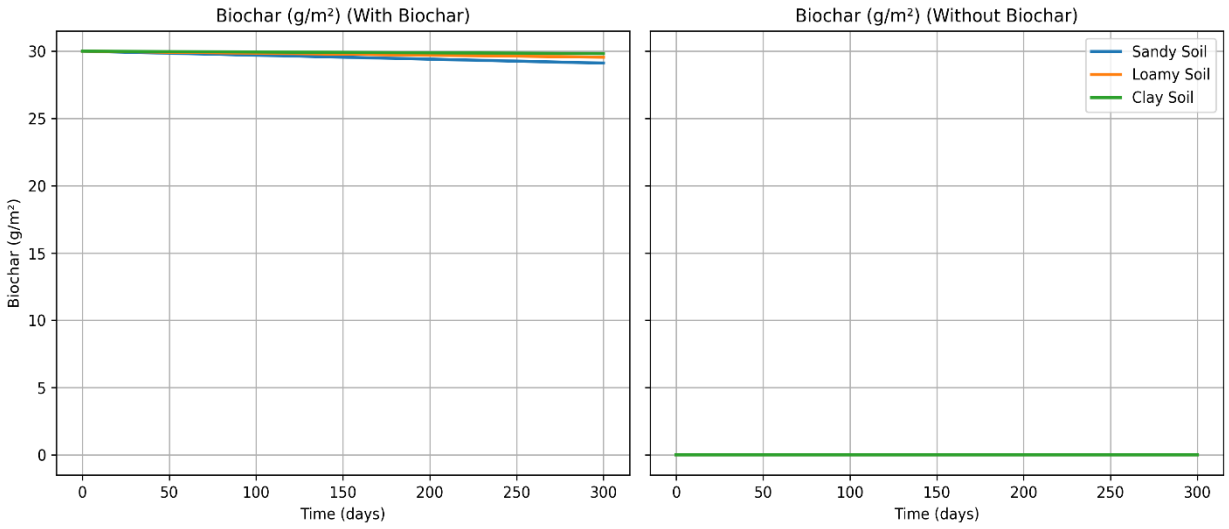

Figure 5:Biochar Persistence (g/m²) in Soil Over 300 Days: BDF-Modeled Trends Showing Slow Decomposition with and without Control

3.6 CROP YIELD (G/M²) ENHANCEMENT WITH BIOCHAR

Figure 6 shows that crop yield increases with biochar because it improves soil nutrients and water retention. Without biochar, yields are lower, particularly in sandy soils with poor nutrient retention.

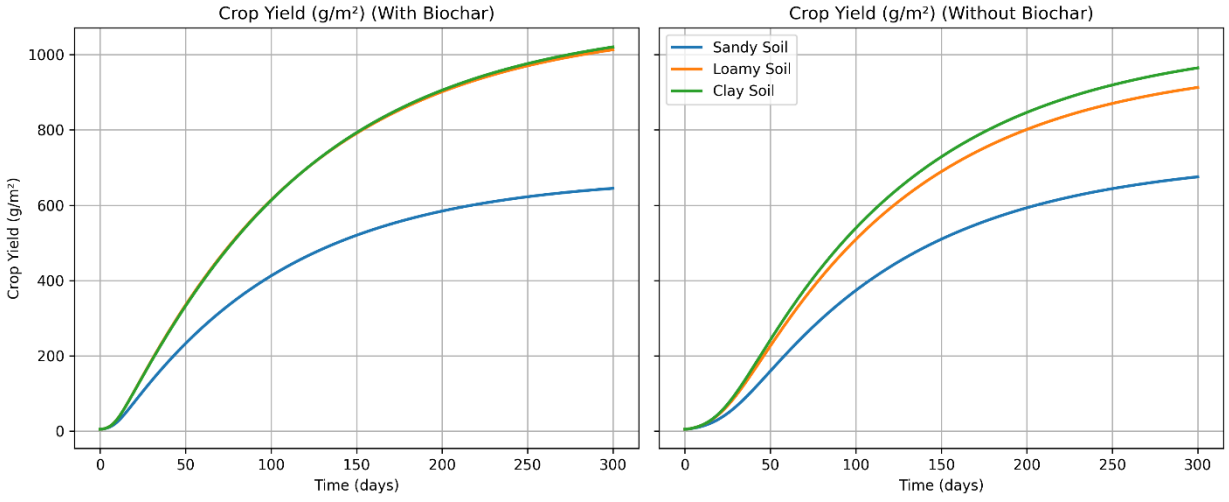

Figure 6:Crop Yield (g/m²) Enhancement with Biochar: BDF Trends Highlight Soil-Specific Benefits

3.7 RESULTS OF SENSITIVITY ANALYSIS

Figure 7 shows the sensitivity analysis results using Morris with the mean elementary effects of the environmental and biological parameters while Figure 8 shows the sensitivity analysis using the Sobol techniques for the first order and sum of the order.

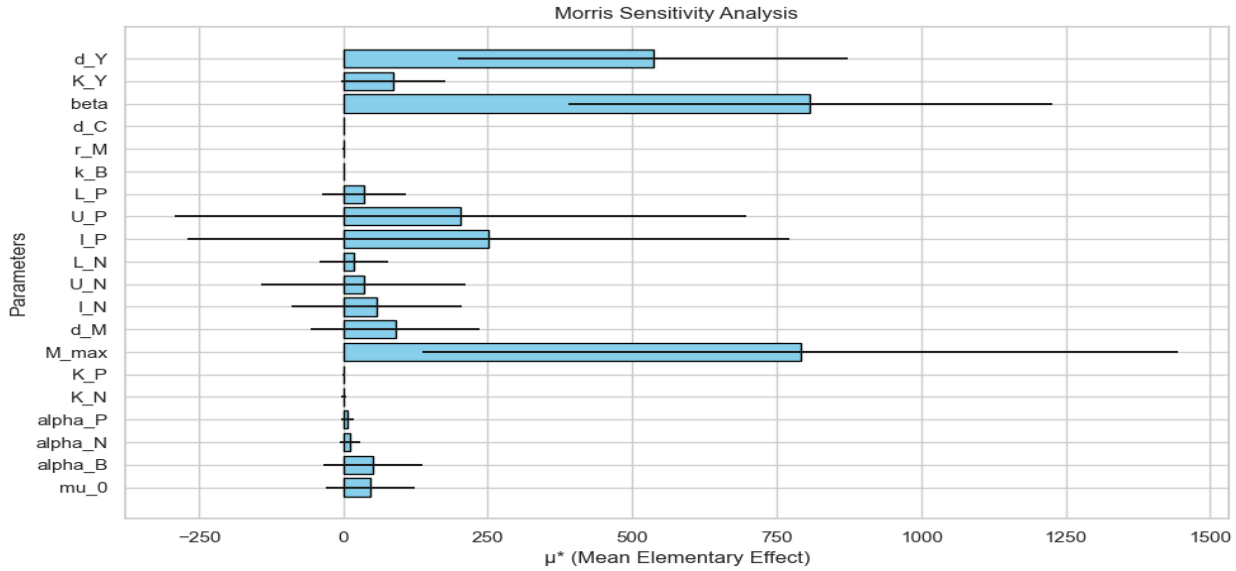

Figure 7:Morris Sensitivity Analysis of Biological and Environmental Parameters

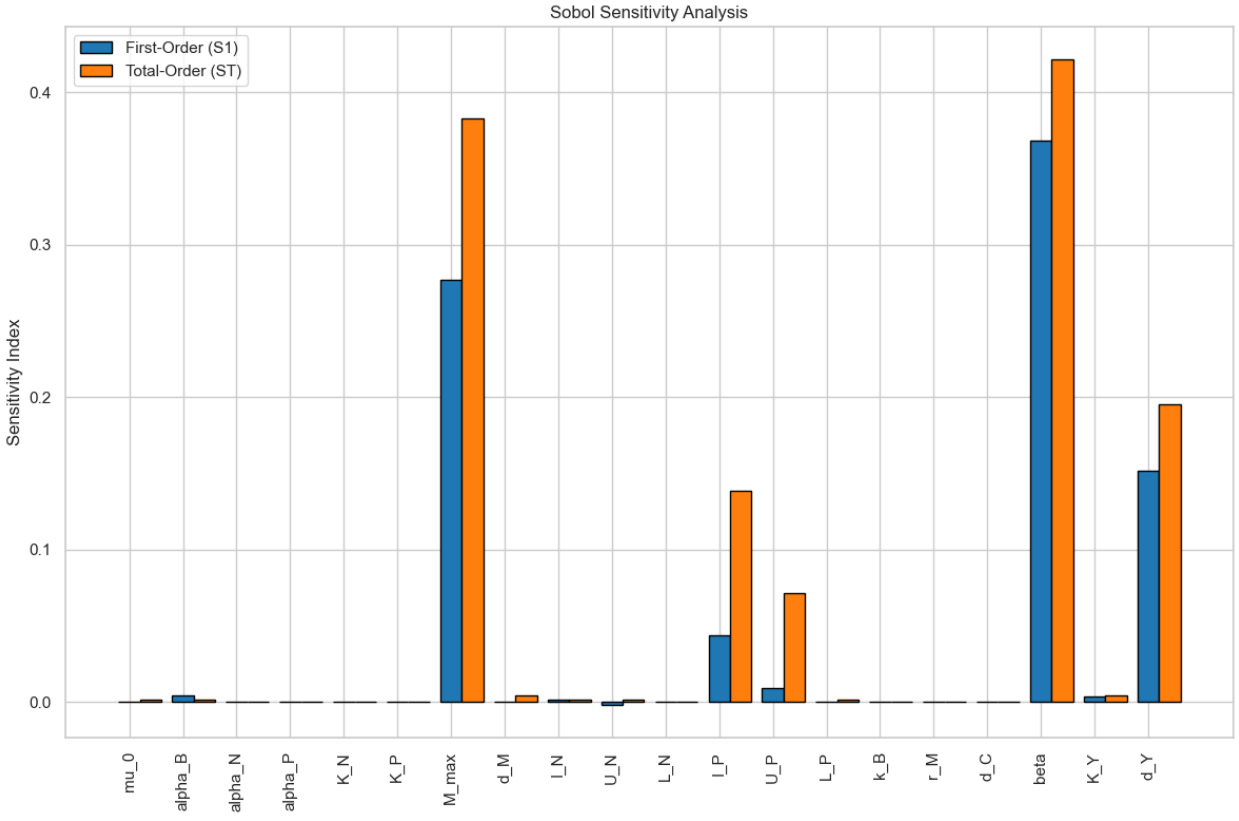

Figure 8: Sobol Sensitivity Analysis for First and Total Order

4. Discussion of Results

Biochar addition reduced crop yield (644.7 versus 964.6 g/m²), nitrogen (105.1 versus 294.1 g N/m²), and phosphorus (9.4 versus 103.9 g P/m²) in sandy soils compared to control treatments (Table 3). This implies that the addition of biochar, at least in this particular case, did not improve these important soil properties and crop performance as anticipated. This is consistent with the findings of [21, 36, 37, 38, 39], which demonstrated that the beneficial effects of biochar on soil fertility and crop yield are not always guaranteed and that they heavily depend on feedstock, the temperature at which biochar is produced, and, most importantly, the type of soil. In contrast, biochar maintained nitrogen levels that were nearly the same as those of the controls (292.3 vs. 294.1 g N/m²) while considerably increasing crop output (1012.8 vs. 964.6 g/m²) and phosphorus availability (149.0 vs. 103.9 g P/m²) in loamy soils. Our results demonstrate the interplay between biochar, nitrogen, and other soil characteristics such as pH and microbial activity, which have a substantial impact on nitrogen availability and plant uptake. Numerous studies have established the positive effects of biochar on nitrogen retention [40, 41, 42, 43]. In clay soils, a particularly compelling pattern emerged: biochar enhanced crop yield (1020.2 vs. 964.6 g/m²) while causing slight drops in phosphorus (99.0 vs. 103.9 g P/m²) and nitrogen (290.0 vs. 294.1 g N/m²). This outcome implies that the impacts of biochar on plant growth might be greatly impacted by its effects on soil physical characteristics, especially in clay-rich soils, and are not only reliant on nutrient retention. This is especially noteworthy because earlier research frequently emphasised the function of biochar in retaining nutrients [44, 45, 46, 47], but this particular finding suggests a more complex relationship in clay-rich settings. This indicates that the enhanced yield is not solely dependent on the overall quantity of nutrients present but also on the improved soil conditions caused by biochar.

The computational resolution demonstrated by the reference model needed 0.27 to 0.50 seconds, depending on the kind of soil in Table 4. On the other hand, every evaluated scheme experienced significant computing time savings; the quickest approach was BDF in every example (0.005–0.018 s), followed by RK4 (0.018–0.036 s) and the Trapezoidal scheme (0.104–0.175 s). Up to two orders of magnitude faster than the reference, BDF's exceptional time efficiency indicates that it is especially well-suited for situations requiring quick simulations, including sensitivity analyses across wide parameter spaces or real-time irrigation control. Loamy soil circumstances exhibited the greatest RMSE for BDF, indicating the presence of mixed-flow regimes due to intermediate

pore-size distributions that are more difficult for the implicit discretisation of the approach to accommodate. Table 5 shows that BDF had slightly lower nitrogen and phosphorus concentrations than the other techniques, while RK4 and Trapezoidal had nearly the same for every variable. Additionally, in line with the greater RMSE previously noted for BDF, the BDF approach produced a marginally lower crop yield (912.69 g/m^2) compared to RK4 (912.90 g/m^2) and Trapezoidal (912.90 g/m^2). While BDF maintained good accuracy despite minor systematic differences in yield and nutrient pools, RK4 and Trapezoidal produced findings that were almost identical overall and had the best agreement with the reference solution.

As shown in Figure 1, the observed increase in microbial biomass in soils treated with biochar indicates that biochar is effectively providing a chemical and physical environment that promotes microbial growth and activity. This is particularly evident in the impact of biochar's alkaline nature and porous structure on microbial communities. This result demonstrates the immediate impacts and processes driving microbial responses to biochar amendment, while previous studies frequently concentrated on the long-term benefits of soil health improvements or specific soil types [48, 49, 50]. However, in non-biochar soils, microbial development was slower, which might have been forced by environmental stressors and competition for resources. This finding is consistent with recent research by Haider et al. [51], who showed that resource competition and environmental stressors in the non-biochar soils may be the cause of delayed microbial development.

The biochar-amended soils exhibit a steeper increase in N, P, and C accumulation (Figure 2-4), indicating less leaching and better mineralisation. This is demonstrated by the characteristics of biochar, including its cation exchange capacity, which keeps ammonium-N in the soil and prevents its loss, and its surface functional groups, which bind phosphate ions and reduce their susceptibility to leaching, so increasing their availability for plant uptake over time. The study's findings are corroborated by evidence of nutrient adsorption and desorption, which show that biochar can store and release nutrients in a way that promotes plant development [52, 53, 54, 55]. The result highlights how biochar significantly increases soil carbon sequestration (Figure 5), which supports the organic matter's resistance [56, 57, 58, 59]. As seen in Figure 6, the beneficial effects of biochar on yield are not solely attributable to direct nutrient provision but also the intricate interactions between biochar, soil microorganisms, and nutrient cycling. As a result, there is a direct correlation between patterns in nutrient availability and the 20% yield difference across

treatments. Consequently, shows the complex interplay between biochar, soil microbes, and nutrient cycling when assessing the effects of biochar on crop yields [59, 60, 61].

Morris measures mean elementary effects, showing which parameters have the biggest impact in Figure 7. The Morris method identified M_{max} (microbial carrying capacity) and β (crop growth efficiency) as the most influential parameters, as evidenced by their high mean elementary effects (μ^*), which indicate strong direct impacts on crop yield. Parameters such as I_P (irrigation parameter) and L_P (light parameter) displayed long horizontal bars, signifying high variability and suggesting significant interactions with other variables. This implies that these variables are dynamic and subject to significant fluctuations, which may be caused by additional variables such as crop type, soil composition, or weather patterns [62, 63]. This variability demands the use of mathematical models, such as modified stencil points for the method of lines [64], Chebyshev differentiation matrices [65], Hermite polynomial-based techniques [66], and radial basis function–finite difference (RBF-FD) approximations [67], to optimise irrigation and light strategies, guaranteeing effective resource allocation and increased crop yields. AI algorithms are also capable of processing data from a variety of sensors, such as weather stations and soil moisture sensors, and modifying light intensity and irrigation schedules in real-time to maximise crop yield while utilising the fewest resources possible [68].

Meanwhile, Sobol breaks down sensitivity into first order (S_1) and total-order (S_T) indices, where S_T includes interactions. In the Sobol analysis, the first-order index (S_1**)** showed M_{max} as the dominant contributor (approximately 0.38), reflecting its substantial standalone effect. The total-order index **(**S_T**)** identified β and d_Y (crop decay rate) as having the highest influence (both around 0.42), indicating their effects are primarily driven by interactions with other parameters. Both sensitivity methods consistently identified M_{max} as the most critical parameter affecting yield. Its high values in both μ^* (Morris) and S_1 (Sobol) reinforce its direct role in regulating microbial biomass and overall crop productivity. The parameter β exhibited a low S_1 but a high S_T in the Sobol method, consistent with its moderate μ^* in the Morris method. This discrepancy suggests that β has limited direct influence but significant interaction effects. Similarly, K_N and K_Y (nutrient half-saturation constants) had low S_1 but moderate S_T values, consistent with their lower μ^*in the Morris analysis, indicating more nuanced, context-dependent roles. Parameters such as α_B (biochar influence on microbial activity) and μ_o (baseline microbial growth rate) demonstrated minimal impact across both sensitivity analyses. Their negligible influence supports

the decision to exclude them from further model refinement. The findings from both Morris and Sobol analyses converge on M_{max} as the primary driver of crop yield within the modeled system. Discrepancies, such as β exhibiting high S_T but moderate μ^* indices in sensitivity analysis is therefore essential for capturing the multifactorial dynamics of agroecosystems. This combined approach enhances the robustness of model simplification and informs the prioritization of parameters for effective agricultural management and decision-making [69, 70, 71].

5. CONCLUSION

This study presents a comprehensive mathematical modelling approach to simulate the interactions among microbial dynamics, nutrient cycling, biochar amendments, and crop productivity in a soil ecosystem. The model incorporates important characteristics that control soil fertility and crop output, including microbial growth and decay rates, nutrient input and leaching rates and the impacts of biochar. We used the BDF, a stiff ODE solver, to solve a model of microbial-nutrient kinetics for soils amended with biochar. Comparative numerical trials against explicit Runge–Kutta and Trapezoidal schemes have demonstrated that BDF outperforms conventional approaches in terms of stability, accuracy, and computational efficiency, particularly under rigid parameter regimes and high time steps. The integration of biochar impact coefficients, microbial respiration, and carbon loss pathways also allows for the evaluation of sustainable agricultural practices, avoiding simplifications, thereby enabling more realistic simulations. From a computational perspective, the BDF framework opens the door for efficient and stable integration of complex biogeochemical systems where stiffness has historically been a limiting factor. The parameter values used in the model reflect realistic agro-ecological conditions, offering a strong foundation for simulating system behaviour under various management scenarios. Although the model took into consideration the growth and decomposition of microbes, it is difficult to accurately represent the complex interactions among the soil microbiome, including competition, cooperation, and pathogen control. We recommend the adoption of BDF-based solvers for similar environmental and ecological modelling problems where stiffness is unavoidable. Future studies should focus on developing machine learning and numerical models that consider the structure of microbial communities, their functional genes, and their interactions with biochar and other soil constituents.

ACKNOWLEDGEMENTS

We appreciate the Management of the Federal Polytechnic Ilaro, the host institution, for affording

us its support through the provision of an enabling environment for the research and funding of the APC.

CONFLICT OF INTERESTS

The authors declare that there is no conflict of interests.

REFERENCES

[1] K.N. Shoudho, T.H. Khan, U.R. Ara, M.R. Khan, Z.B.Z. Shawon, et al., Biochar in Global Carbon Cycle: Towards Sustainable Development Goals, Curr. Res. Green Sustain. Chem. 8 (2024), 100409. https://doi.org/10.1016/j.crgsc.2024.100409.

[2] E. Kabir, K. Kim, E.E. Kwon, Biochar as a Tool for the Improvement of Soil and Environment, Front. Environ. Sci. 11 (2023), 1324533. https://doi.org/10.3389/fenvs.2023.1324533.

[3] S. Shyam, S. Ahmed, S.J. Joshi, H. Sarma, Biochar as a Soil Amendment: Implications for Soil Health, Carbon Sequestration, and Climate Resilience, Discov. Soil 2 (2025), 18. https://doi.org/10.1007/s44378-025-00041-8.

[4] A. Waheed, H. Xu, X. Qiao, A. Aili, Y. Yiremaikebayi, et al., Biochar in Sustainable Agriculture and Climate Mitigation: Mechanisms, Challenges, and Applications in the Circular Bioeconomy, Biomass- Bioenergy 193 (2025), 107531. https://doi.org/10.1016/j.biombioe.2024.107531.

[5] L.C.A. Melo, M.Á. Sánchez-Monedero, How Biochar-Based Fertilizers and Biochar Compost Affect Nutrient Cycling and Crop Productivity, Nutr. Cycl. Agroecosystems 128 (2024), 411-414. https://doi.org/10.1007/s10705-024-10358-5.

[6] A. Ali, N. Jabeen, Z. Chachar, S. Chachar, S. Ahmed, et al., The Role of Biochar in Enhancing Soil Health & Interactions with Rhizosphere Properties and Enzyme Activities in Organic Fertilizer Substitution, Front. Plant Sci. 16 (2025), 1595208. https://doi.org/10.3389/fpls.2025.1595208.

[7] J.A. Antonangelo, X. Sun, H.D.J. Eufrade-Junior, Biochar Impact on Soil Health and Tree-Based Crops: A Review, Biochar 7 (2025), 51. https://doi.org/10.1007/s42773-025-00450-6.

[8] H. Li, E.S. Azzi, C. Sundberg, E. Karltun, H. Cederlund, Can Inert Pool Models Improve Predictions of Biochar Long-Term Persistence in Soils?, Geoderma 452 (2024), 117093. https://doi.org/10.1016/j.geoderma.2024.117093.

[9] J.K.M. Chagas, C.C.D. Figueiredo, M.L.G. Ramos, Biochar Increases Soil Carbon Pools: Evidence from a Global Meta-Analysis, J. Environ. Manag. 305 (2022), 114403. https://doi.org/10.1016/j.jenvman.2021.114403.

[10] Imran, Amanullah, A.R.M. Al-Tawaha, Carbon Sources Application Increase Wheat Yield and Soil Fertility, Commun. Soil Sci. Plant Anal. 52 (2021), 695-703. https://doi.org/10.1080/00103624.2020.1865397.

[11] N. Sun, B. Sarkar, S. Li, Y. Tian, L. Sha, et al., Biochar Addition Increased Soil Carbon Storage but Did Not Exacerbate Soil Carbon Emission in Young Subtropical Plantation Forest, Forests 15 (2024), 917. https://doi.org/10.3390/f15060917.

[12] L. Menichetti, G.I. Ågren, P. Barré, F. Moyano, T. Kätterer, Generic Parameters of First-Order Kinetics Accurately Describe Soil Organic Matter Decay in Bare Fallow Soils Over a Wide Edaphic and Climatic Range,

Sci. Rep. 9 (2019), 20319. https://doi.org/10.1038/s41598-019-55058-1.

[13] A.K. Chandel, L. Jiang, Y. Luo, Microbial Models for Simulating Soil Carbon Dynamics: A Review, J. Geophys. Res.: Biogeosciences 128 (2023), e2023JG007436. https://doi.org/10.1029/2023jg007436.

[14] G. Lanza, A. Stang, J. Kern, S. Wirth, A. Gessler, Degradability of Raw and Post-Processed Chars in a Two-Year Field Experiment, Sci. Total. Environ. 628-629 (2018), 1600-1608. https://doi.org/10.1016/j.scitotenv.2018.02.164.

[15] J.R. Ridgeway, E.M. Morrissey, E.R. Brzostek, Plant Litter Traits Control Microbial Decomposition and Drive Soil Carbon Stabilization, Soil Biol. Biochem. 175 (2022), 108857. https://doi.org/10.1016/j.soilbio.2022.108857.

[16] X. Zhang, Z. Xie, Z. Ma, G.A. Barron-Gafford, R.L. Scott, et al., A Microbial‐Explicit Soil Organic Carbon Decomposition Model (MESDM): Development and Testing at a Semiarid Grassland Site, J. Adv. Model. Earth Syst. 14 (2022), e2021MS002485. https://doi.org/10.1029/2021ms002485.

[17] C. Wang, X. Wang, Y. Zhang, E. Morrissey, Y. Liu, et al., Integrating Microbial Community Properties, Biomass and Necromass to Predict Cropland Soil Organic Carbon, ISME Commun. 3 (2023), 86. https://doi.org/10.1038/s43705-023-00300-1.

[18] J. Tang, W.J. Riley, Finding Liebig's Law of the Minimum, Ecol. Appl. 31 (2021), e02458. https://doi.org/10.1002/eap.2458.

[19] T. Van Daele, S. Van Hoey, I. Nopens, pyIDEAS: An Open Source Python Package for Model Analysis, Comput. Aided Chem. Eng. 37 (2015), 569-574. https://doi.org/10.1016/b978-0-444-63578-5.50090-6.

[20] J.B. Morgan, E.L. Connolly, Plant-Soil Interactions: Nutrient Uptake, Nat. Educ. Knowl. 4 (2013), 2.

[21] S. Abel, A. Peters, S. Trinks, H. Schonsky, M. Facklam, et al., Impact of Biochar and Hydrochar Addition on Water Retention and Water Repellency of Sandy Soil, Geoderma 202-203 (2013), 183-191. https://doi.org/10.1016/j.geoderma.2013.03.003.

[22] S.D. Allison, M.D. Wallenstein, M.A. Bradford, Soil-Carbon Response to Warming Dependent on Microbial Physiology, Nat. Geosci. 3 (2010), 336-340. https://doi.org/10.1038/ngeo846.

[23] J. Lehmann, M.C. Rillig, J. Thies, C.A. Masiello, W.C. Hockaday, et al., Biochar Effects on Soil Biota – A Review, Soil Biol. Biochem. 43 (2011), 1812-1836. https://doi.org/10.1016/j.soilbio.2011.04.022.

[24] A.R. Zimmerman, B. Gao, M. Ahn, Positive and Negative Carbon Mineralization Priming Effects among a Variety of Biochar-Amended Soils, Soil Biol. Biochem. 43 (2011), 1169-1179. https://doi.org/10.1016/j.soilbio.2011.02.005.

[25] J. Schimel, The Implications of Exoenzyme Activity on Microbial Carbon and Nitrogen Limitation in Soil: A Theoretical Model, Soil Biol. Biochem. 35 (2003), 549-563. https://doi.org/10.1016/s0038-0717(03)00015-4.

[26] B.L. Turner, P.M. Haygarth, Phosphatase Activity in Temperate Pasture Soils: Potential Regulation of Labile Organic Phosphorus Turnover by Phosphodiesterase Activity, Sci. Total. Environ. 344 (2005), 27-36. https://doi.org/10.1016/j.scitotenv.2005.02.003.

[27] E.A. Davidson, S. Samanta, S.S. Caramori, K. Savage, The Dual Arrhenius and Michaelis–Menten Kinetics Model for Decomposition of Soil Organic Matter at Hourly to Seasonal Time Scales, Glob. Chang. Biol. 18

(2011), 371-384. https://doi.org/10.1111/j.1365-2486.2011.02546.x.

[28] P.M. Vitousek, J.D. Aber, R.W. Howarth, G.E. Likens, P.A. Matson, et al., Human Alteration of the Global Nitrogen Cycle: Sources and Consequences, Ecol. Appl. 7 (1997), 737-750. https://doi.org/10.1890/1051-0761(1997)007[0737:haotgn]2.0.co;2.

[29] J.N. Galloway, A.R. Townsend, J.W. Erisman, M. Bekunda, Z. Cai, et al., Transformation of the Nitrogen Cycle: Recent Trends, Questions, and Potential Solutions, Science 320 (2008), 889-892. https://doi.org/10.1126/science.1136674.

[30] J.J. Elser, M.E. Bracken, E.E. Cleland, D.S. Gruner, W.S. Harpole, et al., Global Analysis of Nitrogen and Phosphorus Limitation of Primary Producers in Freshwater, Marine and Terrestrial Ecosystems, Ecol. Lett. 10 (2007), 1135-1142. https://doi.org/10.1111/j.1461-0248.2007.01113.x.

[31] Y. Kuzyakov, I. Subbotina, H. Chen, I. Bogomolova, X. Xu, Black Carbon Decomposition and Incorporation into Soil Microbial Biomass Estimated by 14C Labeling, Soil Biol. Biochem. 41 (2009), 210-219. https://doi.org/10.1016/j.soilbio.2008.10.016.

[32] S. Fontaine, S. Barot, P. Barré, N. Bdioui, B. Mary, et al., Stability of Organic Carbon in Deep Soil Layers Controlled by Fresh Carbon Supply, Nature 450 (2007), 277-280. https://doi.org/10.1038/nature06275.

[33] K.J. van Groenigen, C.W. Osenberg, B.A. Hungate, Increased Soil Emissions of Potent Greenhouse Gases Under Increased Atmospheric CO2, Nature 475 (2011), 214-216. https://doi.org/10.1038/nature10176.

[34] D.B. Lobell, W. Schlenker, J. Costa-Roberts, Climate Trends and Global Crop Production Since 1980, Science 333 (2011), 616-620. https://doi.org/10.1126/science.1204531.

[35] D. Tilman, K.G. Cassman, P.A. Matson, R. Naylor, S. Polasky, Agricultural Sustainability and Intensive Production Practices, Nature 418 (2002), 671-677. https://doi.org/10.1038/nature01014.

[36] S. Gul, J.K. Whalen, B.W. Thomas, V. Sachdeva, H. Deng, Physico-Chemical Properties and Microbial Responses in Biochar-Amended Soils: Mechanisms and Future Directions, Agric. Ecosyst. Environ. 206 (2015), 46-59. https://doi.org/10.1016/j.agee.2015.03.015.

[37] A. El-Naggar, S.S. Lee, J. Rinklebe, M. Farooq, H. Song, et al., Biochar Application to Low Fertility Soils: A Review of Current Status, and Future Prospects, Geoderma 337 (2019), 536-554. https://doi.org/10.1016/j.geoderma.2018.09.034.

[38] M. Hussain, M. Farooq, A. Nawaz, A.M. Al-Sadi, Z.M. Solaiman, et al., Biochar for Crop Production: Potential Benefits and Risks, J. Soils Sediments 17 (2016), 685-716. https://doi.org/10.1007/s11368-016-1360-2.

[39] Y. Ding, Y. Liu, S. Liu, Z. Li, X. Tan, et al., Biochar to Improve Soil Fertility. A Review, Agron. Sustain. Dev. 36 (2016), 36. https://doi.org/10.1007/s13593-016-0372-z.

[40] S. Bolan, D. Hou, L. Wang, L. Hale, D. Egamberdieva, et al., The Potential of Biochar as a Microbial Carrier for Agricultural and Environmental Applications, Sci. Total. Environ. 886 (2023), 163968. https://doi.org/10.1016/j.scitotenv.2023.163968.

[41] C. Tu, J. Wei, F. Guan, Y. Liu, Y. Sun, et al., Biochar and Bacteria Inoculated Biochar Enhanced Cd and Cu Immobilization and Enzymatic Activity in a Polluted Soil, Environ. Int. 137 (2020), 105576. https://doi.org/10.1016/j.envint.2020.105576.

[42] X. Zhang, H. Wang, L. He, K. Lu, A. Sarmah, et al., Using Biochar for Remediation of Soils Contaminated with Heavy Metals and Organic Pollutants, Environ. Sci. Pollut. Res. 20 (2013), 8472-8483. https://doi.org/10.1007/s11356-013-1659-0.

[43] X. Zhang, Z. Gong, G. Allinson, X. Li, C. Jia, Joint Effects of Bacterium and Biochar in Remediation of Antibiotic-Heavy Metal Contaminated Soil and Responses of Resistance Gene and Microbial Community, Chemosphere 299 (2022), 134333. https://doi.org/10.1016/j.chemosphere.2022.134333.

[44] Z.X. Jiang, S. Cui, X. Zhang, M. Xi, D.M. Sun, Influence of Biochar Application on Soil Nitrate Leaching and Phosphate Retention: A Synthetic Meta-Analysis, Huan Jing ke Xue 43 (2022), 4658–4668. https://doi.org/10.13227/j.hjkx.202112314.

[45] E. Kabir, K. Kim, E.E. Kwon, Biochar as a Tool for the Improvement of Soil and Environment, Front. Environ. Sci. 11 (2023), 1324533. https://doi.org/10.3389/fenvs.2023.1324533.

[46] S. Khan, S. Irshad, K. Mehmood, Z. Hasnain, M. Nawaz, et al., Biochar Production and Characteristics, Its Impacts on Soil Health, Crop Production, and Yield Enhancement: A Review, Plants 13 (2024), 166. https://doi.org/10.3390/plants13020166.

[47] D. Wang, P. Jiang, H. Zhang, W. Yuan, Biochar Production and Applications in Agro and Forestry Systems: A Review, Sci. Total. Environ. 723 (2020), 137775. https://doi.org/10.1016/j.scitotenv.2020.137775.

[48] K.N. Palansooriya, J.T.F. Wong, Y. Hashimoto, L. Huang, J. Rinklebe, et al., Response of Microbial Communities to Biochar-Amended Soils: A Critical Review, Biochar 1 (2019), 3-22. https://doi.org/10.1007/s42773-019-00009-2.

[49] Y. Wen, R. Wu, D. Qi, T. Xu, W. Chang, et al., The Effect of AMF Combined with Biochar on Plant Growth and Soil Quality Under Saline-Alkali Stress: Insights from Microbial Community Analysis, Ecotoxicol. Environ. Saf. 281 (2024), 116592. https://doi.org/10.1016/j.ecoenv.2024.116592.

[50] K. He, G. He, C. Wang, H. Zhang, Y. Xu, et al., Biochar Amendment Ameliorates Soil Properties and Promotes Miscanthus Growth in a Coastal Saline-Alkali Soil, Appl. Soil Ecol. 155 (2020), 103674. https://doi.org/10.1016/j.apsoil.2020.103674.

[51] F.U. Haider, X. Wang, U. Zulfiqar, M. Farooq, S. Hussain, et al., Biochar Application for Remediation of Organic Toxic Pollutants in Contaminated Soils; an Update, Ecotoxicol. Environ. Saf. 248 (2022), 114322. https://doi.org/10.1016/j.ecoenv.2022.114322.

[52] A.M. Zubairu, E. Michéli, C.M. Ocansey, N. Boros, G. Rétháti, et al., Biochar Improves Soil Fertility and Crop Performance: A Case Study of Nigeria, Soil Syst. 7 (2023), 105. https://doi.org/10.3390/soilsystems7040105.

[53] Z. Hamidzadeh, P. Ghorbannezhad, M.R. Ketabchi, B. Yeganeh, Biomass-Derived Biochar and Its Application in Agriculture, Fuel 341 (2023), 127701. https://doi.org/10.1016/j.fuel.2023.127701.

[54] M. Awodun, S. Oladele, A. Adeyemo, Efficient Nutrient Use and Plant Probiotic Microbes Interaction, in: V. Kumar, M. Kumar, S. Sharma, R. Prasad (Eds.), Probiotics in Agroecosystem, Springer, Singapore, 2017: pp. 217–232. https://doi.org/10.1007/978-981-10-4059-7_12.

[55] F. Obi, B. Ugwuishiwu, J. Nwakaire, Agricultural Waste Concept, Generation, Utilization and Management, Niger. J. Technol. 35 (2016), 957-964. https://doi.org/10.4314/njt.v35i4.34.

[56] K.A. Spokas, Review of the Stability of Biochar in Soils: Predictability of O:C Molar Ratios, Carbon Manag. 1 (2010), 289-303. https://doi.org/10.4155/cmt.10.32.

[57] J. Wang, Z. Xiong, Y. Kuzyakov, Biochar Stability in Soil: Meta‐Analysis of Decomposition and Priming Effects, GCB Bioenergy 8 (2015), 512-523. https://doi.org/10.1111/gcbb.12266.

[58] B. Ernest, P.Z. Yanda, A. Hansson, M. Fridahl, Long-Term Effects of Adding Biochar to Soils on Organic Matter Content, Persistent Carbon Storage, and Moisture Content in Karagwe, Tanzania, Sci. Rep. 14 (2024), 30565. https://doi.org/10.1038/s41598-024-83372-w.

[59] M.R. Patel, N.L. Panwar, Biochar from Agricultural Crop Residues: Environmental, Production, and Life Cycle Assessment Overview, Resour. Conserv. Recycl. Adv. 19 (2023), 200173. https://doi.org/10.1016/j.rcradv.2023.200173.

[60] P. Khare, Y. Deshmukh, V. Yadav, V. Pandey, A. Singh, et al., Biochar Production: A Sustainable Solution for Crop Residue Burning and Related Environmental Issues, Environ. Prog. Sustain. Energy 40 (2020), e13529. https://doi.org/10.1002/ep.13529.

[61] A. Ali, N. Jabeen, Z. Chachar, S. Chachar, S. Ahmed, et al., The Role of Biochar in Enhancing Soil Health & Interactions with Rhizosphere Properties and Enzyme Activities in Organic Fertilizer Substitution, Front. Plant Sci. 16 (2025), 1595208. https://doi.org/10.3389/fpls.2025.1595208.

[62] D. Zwicker, L. Laan, Evolved Interactions Stabilize Many Coexisting Phases in Multicomponent Liquids, Proc. Natl. Acad. Sci. 119 (2022), e2201250119. https://doi.org/10.1073/pnas.2201250119.

[63] D. Maria Manuel Vianny, A. John, S. Kumar Mohan, A. Sarlan, Adimoolam, et al., Water Optimization Technique for Precision Irrigation System Using IoT and Machine Learning, Sustain. Energy Technol. Assessments 52 (2022), 102307. https://doi.org/10.1016/j.seta.2022.102307.

[64] F.M. Okafor, M.O. Durojaye, J.K. Odeyemi, B.G. Ogunware, A Comparative Study of Stencil-Based Method of Lines for Solving the Burgers-Huxley Equation, FUDMA J. Sci. 9 (2025), 1-7. https://doi.org/10.33003/fjs-2025-0907-3742.

[65] M.O. Durojaye, J.K. Odeyemi, I.J. Ajie, Numerical Solution of Two Dimensional Laplace's Equation on a Regular Domain Using Chebyshev Differentiation Matrices, Phys. Sci. Int. J. 23 (2019), 1-7. https://doi.org/10.9734/psij/2019/v23i130144.

[66] J.K. Odeyemi, O.O. Olaiya, F.O. Ogunfiditimi, Hermite Polynomial-Based Methods for Optimal Order Approximation of First-Order Ordinary Differential Equations, J. Adv. Math. Comput. Sci. 38 (2023), 16-32. https://doi.org/10.9734/jamcs/2023/v38i61765.

[67] M.O. Durojaye, J.K. Odeyemi, Radial Basis Function–Finite Difference (RBF-FD) Approximations for Two-Dimensional Heat Equations, Pac. J. Sci. Technol. 20 (2019), 43–49.

[68] N.C. Gaitan, B.I. Batinas, C. Ursu, F.N. Crainiciuc, Integrating Artificial Intelligence into an Automated Irrigation System, Sensors 25 (2025), 1199. https://doi.org/10.3390/s25041199.

[69] R. Confalonieri, G. Bellocchi, S. Tarantola, M. Acutis, M. Donatelli, et al., Sensitivity Analysis of the Rice Model WARM in Europe: Exploring the Effects of Different Locations, Climates and Methods of Analysis on Model Sensitivity to Crop Parameters, Environ. Model. Softw. 25 (2010), 479-488. https://doi.org/10.1016/j.envsoft.2009.10.005.

[70] M.P.G. de Oliveira, T.Q. Zorzeto-Cesar, R.D.S. Nóia Júnior, D. Wallach, S. Asseng, et al., Uncertainty in Greenhouse Tomato Growth Models, Comput. Electron. Agric. 225 (2024), 109324. https://doi.org/10.1016/j.compag.2024.109324.

[71] K.C. DeJonge, J.C. Ascough, M. Ahmadi, A.A. Andales, M. Arabi, Global Sensitivity and Uncertainty Analysis of a Dynamic Agroecosystem Model Under Different Irrigation Treatments, Ecol. Model. 231 (2012), 113-125. https://doi.org/10.1016/j.ecolmodel.2012.01.024.

[72] S. Manzoni, P. Taylor, A. Richter, A. Porporato, G.I. Ågren, Environmental and Stoichiometric Controls on Microbial Carbon‐use Efficiency in Soils, New Phytol. 196 (2012), 79-91. https://doi.org/10.1111/j.1469-8137.2012.04225.x.

[73] B. Wang, S.D. Allison, Emergent Properties of Organic Matter Decomposition by Soil Enzymes, Soil Biol. Biochem. 136 (2019), 107522. https://doi.org/10.1016/j.soilbio.2019.107522.

[74] I. Shojaei, N. Arjmand, B. Bazrgari, An Optimization‐based Method for Prediction of Lumbar Spine Segmental Kinematics from the Measurements of Thorax and Pelvic Kinematics, Int. J. Numer. Methods Biomed. Eng. 31 (2015), e02729. https://doi.org/10.1002/cnm.2729.

[75] S.V. Archontoulis, I. Huber, F.E. Miguez, P.J. Thorburn, N. Rogovska, et al., A Model for Mechanistic and System Assessments of Biochar Effects on Soils and Crops and Trade‐offs, GCB Bioenergy 8 (2016), 1028-1045. https://doi.org/10.1111/gcbb.12314.

[76] A. Ronix, E.C. da Silva Neto, C.E.P. Cerri, A.E. Latawiec, J.L.N. Carvalho, Incorporating Biochar into Biogeochemical Models: Achievements and Challenges, GCB Bioenergy 17 (2025), e70037. https://doi.org/10.1111/gcbb.70037.

[77] O. Anyebe, F.K. Sadiq, B.O. Manono, T.A. Matsika, Biochar Characteristics and Application: Effects on Soil Ecosystem Services and Nutrient Dynamics for Enhanced Crop Yields, Nitrogen 6 (2025), 31. https://doi.org/10.3390/nitrogen6020031.

[78] D.S. Powlson, P. Smith, J.U. Smith, eds., Evaluation of Soil Organic Matter Models: Using Existing Long-Term Datasets, Springer, Berlin, Heidelberg, 1996. https://doi.org/10.1007/978-3-642-61094-3.

[79] J. Zimmermann, R. Carolan, P. Forrestal, M. Harty, G. Lanigan, et al., Assessing the Performance of Three Frequently Used Biogeochemical Models When Simulating N2O Emissions from a Range of Soil Types and Fertiliser Treatments, Geoderma 331 (2018), 53-69. https://doi.org/10.1016/j.geoderma.2018.06.004.

[80] C. Li, A. Mosier, R. Wassmann, Z. Cai, X. Zheng, et al., Modeling Greenhouse Gas Emissions from Rice-Based Production Systems: Sensitivity and Upscaling, Glob. Biogeochem. Cycles 18 (2004), 2003GB002045. https://doi.org/10.1029/2003gb002045.

[81] M.D. Morris, Factorial Sampling Plans for Preliminary Computational Experiments, Technometrics 33 (1991), 161-174. https://doi.org/10.1080/00401706.1991.10484804.

[82] I. Sobol′, Global Sensitivity Indices for Nonlinear Mathematical Models and Their Monte Carlo Estimates, Math. Comput. Simul. 55 (2001), 271-280. https://doi.org/10.1016/s0378-4754(00)00270-6.

[83] A. Saltelli, M. Ratto, T. Andres, F. Campolongo, J. Cariboni, et al., Global Sensitivity Analysis. The Primer, Wiley, 2007. https://doi.org/10.1002/9780470725184.

[84] Olusegun Adeyemi Olaiju, Mathematical Modelling of Cholera Transmission Incorporating Open Defecation as an Environmental Driver: An Optimal Control Approach, Int. J. Appl. Math. 38 (2025), 997-1020. https://doi.org/10.12732/ijam.v38i1s.58.

[85] E. Pisoni, D. Albrecht, T. Mara, R. Rosati, S. Tarantola, et al., Application of Uncertainty and Sensitivity Analysis to the Air Quality SHERPA Modelling Tool, Atmospheric Environ. 183 (2018), 84-93. https://doi.org/10.1016/j.atmosenv.2018.04.006.

[86] Y. Fu, L.W. de Jonge, P. Moldrup, M. Paradelo, E. Arthur, Improvements in Soil Physical Properties After Long-Term Manure Addition Depend on Soil and Crop Type, Geoderma 425 (2022), 116062. https://doi.org/10.1016/j.geoderma.2022.116062.

[87] C. Liang, M. Kästner, R.G. Joergensen, Microbial Necromass on the Rise: The Growing Focus on Its Role in Soil Organic Matter Development, Soil Biol. Biochem. 150 (2020), 108000. https://doi.org/10.1016/j.soilbio.2020.108000.